

FORMATION OF OBSCURING WALLS BY THE RADIATION FORCE FROM CIRCUMNUCLEAR STARBURSTS AND THE IMPLICATIONS FOR THE STARBURST–ACTIVE GALACTIC NUCLEUS CONNECTION

KEN OHSUGA AND MASAYUKI UMEMURA

Center for Computational Physics, University of Tsukuba, Tsukuba, Ibaraki 305-8577, Japan

Received 2000 June 23; accepted 2001 May 25

ABSTRACT

We explore the formation of dusty gas walls induced by a circumnuclear starburst around an active galactic nucleus (AGN). We concentrate our attention on the role of the radiation force of a starburst as well as an AGN, in which the effects of the optical depth of dusty gas are taken into consideration. First, we solve the hydrostatic equations in spherical symmetry coupled with the frequency-dependent radiative processes to demonstrate that a geometrically thin, optically thick wall forms because of the radiation pressure of a circumnuclear starburst. Next, in two-dimensional axisymmetric space, we analyze the configuration and the stability of geometrically thin walls that are balanced between radiation pressure and gravity. As a result, it is shown that the radiation force of the circumnuclear starburst works to stabilize optically thick walls surrounding the nucleus. In the case of a brighter starburst with a fainter AGN (e.g., $L_{\text{SB}}/M_{\text{SB}} \gtrsim 10 [L_{\odot}/M_{\odot}]$ and $L_{\text{AGN}} \lesssim 10^{11} L_{\odot}$), there form double walls, the inner one of which is located between the nucleus and the circumnuclear starburst and the outer one of which enshrouds both the starburst regions and the nucleus. The total extinction of both walls turns out to be larger for a brighter starburst, which is $A_V \sim 10$ mag for $L_{\text{SB}}/M_{\text{SB}} \gtrsim 10^2 (L_{\odot}/M_{\odot})$. As a consequence, double walls could heavily obscure the nucleus to make this a type 2 AGN. The outer wall may provide an explanation for the recent indications for large-scale obscuring materials in Seyfert 2 galaxies. Also, it is predicted that the AGN type is time-dependent according to the stellar evolution in the starburst, which shifts from type 2 to type 1 in several times 10^7 yr owing to the disappearance of walls. In contrast, if the AGN itself is much brighter than the starburst, as a quasar is, then neither wall forms regardless of the starburst activity, and the nucleus is likely to be identified as type 1. To conclude, the radiatively supported gas walls could be responsible for the putative correlation between AGN type and the starbursts, whereby Seyfert 2 galaxies are more frequently associated with circumnuclear starbursts than type 1 galaxies, whereas quasars are mostly observed as type 1 AGNs regardless of the star-forming activity in the host galaxies.

Subject headings: galaxies: active — galaxies: evolution — galaxies: nuclei — galaxies: starburst — quasars: general — radiative transfer

1. INTRODUCTION

There has been a good deal of evidence on an obscuring torus of subparsec scale that surrounds an active galactic nucleus (AGN; Antonucci 1984; Wilson, Ward, & Haniff 1988; Barthel 1989; Blanco, Ward, & Wright 1990; Miller & Goodrich 1990; Awaki et al. 1991; Storchi-Bergmann, Mulchaey, & Wilson 1992). The obscuring torus is thought to be responsible for the dichotomy of the AGN type in the context of the unified model (see Antonucci 1993 for a review). However, the origin and physical structure of the torus have not been well elucidated, although some intriguing models are proposed by Krolik & Begelman (1988), Pier & Krolik (1992a, 1992b, 1993), Efstathiou & Rowan-Robinson (1995), and Manske, Henning, & Men'shchikov (1998).

Recent observations on AGN hosts have gradually revealed that the properties of host galaxies of Seyfert nuclei are intrinsically different between type 1 and type 2 AGNs (Heckman et al. 1989; Maiolino et al. 1995, 1997, 1998a; Pérez-Olea & Colina 1996; Hunt et al. 1997; Malkan, Gorjian, & Tam 1998; Storchi-Bergmann, Schmitt, & Fernandes 1999; Storchi-Bergmann et al. 2000; González Delgado, Heckman, & Leitherer 2001). The Seyfert 2 galaxies are more frequently associated with the circumnuclear starbursts than type 1 galaxies. In contrast,

quasars (QSOs) are mostly observed as type 1 AGNs, although the QSO hosts often exhibit vigorous star formation activity (Barvainis, Antonucci, & Coleman 1992; Ohta et al. 1996; Omont et al. 1996; Schinnerer, Eckart, & Tacconi 1998; Brotherton et al. 1999; Canalizo & Stockton 2000a, 2000b; Dietrich & Wilhelm-Erkens 2000). (It is noted that the QSO hosts are fainter than QSO nuclei themselves [McLeod & Rieke 1995b; Bahcall et al. 1997; Hooper, Impey, & Foltz 1997; Crawford et al. 1999; Kirhakos et al. 1999; McLure et al. 1999; McLure, Dunlop, & Kukula 2000].) Such a correlation with circumnuclear starbursts seems beyond understanding based on the picture of the unified model in which the bifurcation of AGN type is simply accounted for by the orientation of the nucleus surrounded by an obscuring torus.

We have some significant pieces of information about the obscuring materials. From X-ray observations, it is indicated that most Seyfert 2 nuclei are heavily obscured along the line of sight with at least $A_V > 10$ and sometimes $A_V > 100$ mag (Matt et al. 1996, 1999; Maiolino et al. 1998b; Bassani et al. 1999; Risaliti, Maiolino, & Salvati 1999). On the other hand, the A_V of the nuclear or circumnuclear regions is estimated to be between a few and several magnitudes by IR and optical observations (Rix et al. 1990; Roche et al. 1991; Goodrich, Veilleux, & Hill 1994; McLeod &

Rieke 1995a; Oliva, Marconi, & Moorwood 1999). Also, it is argued that a component of the obscuring materials must be extended up to ≥ 100 pc in addition to a compact component being confined to subparsec scales (Rudy, Cohen, & Ake 1988; Miller, Goodrich, & Mathews 1991; Goodrich 1995; McLeod & Rieke 1995a; Maiolino et al. 1995; Maiolino & Rieke 1995; Malkan et al. 1998). These facts may suggest that the distributions of dusty gas around an AGN are much more diverse than previously considered and that they have a close relationship with circumnuclear starburst events.

Recently, Ohsuga & Umemura (1999, hereafter Paper I) have suggested a novel picture for the starburst-AGN connection in which a large-scale dusty wall of several hundred parsecs is built up because of the radiation force of a circumnuclear starburst as well as an AGN. This model provides the possibility that the AGN type is regulated by circumnuclear starbursts, and it also gives a physical origin for extended obscuring materials. However, the dusty wall was analyzed in an optically thin regime. Thus, the possibility of the strong obscuration with $A_V \gg 1$ is still an open question in this picture.

In this paper, by taking the optical depth of dusty gas into consideration, we consider the effects of radiation force from a circumnuclear starburst as well as an AGN and investigate the stable configuration of dusty gas. To begin with, we solve hydrostatic equations coupled with the frequency-dependent radiative processes assuming spherical symmetry. From this analysis, we demonstrate that a geometrically thin, optically thick wall forms because of radiation pressure from a starburst. Next, we obtain the stable equilibrium configuration of dusty gas walls in two-dimensional axisymmetric space. Finally, we attempt to classify the AGN type according to the starburst luminosity and the AGN luminosity. Moreover, taking into account the stellar evolution in starburst regions, we discuss the time evolution of the circumnuclear structure. In § 2, the radiation fields and gravitational fields are modeled. In § 3, the structure of a dusty wall is analyzed in a spherically symmetric approximation, demonstrating that a geometrically thin, optically thick wall can form because of radiation force from a starburst. In § 4, the configuration of dusty gas in two-dimensional axisymmetric space is investigated with an approximation of geometrically thin walls, and the conditions for the wall formation are given. In § 5, based on the present picture, we discuss the implications for the starburst-AGN connection. Furthermore, the evolution of AGN type that is predicted by the formation of the obscuring walls is shown in § 6. Section 7 is devoted to conclusions.

2. RADIATION FIELDS AND GRAVITATIONAL FIELDS

Recent observations have revealed that the circumnuclear starburst regions frequently exhibit ringlike features (Wilson et al. 1991; Forbes et al. 1994; Marconi et al. 1994; Mauder et al. 1994; Buta, Purcell, & Crocker 1995; Barth et al. 1995; Leitherer et al. 1996; Maoz et al. 1996; Storchi-Bergman, Wilson, & Baldwin 1996). Therefore, as a component of radiation sources, we assume a starburst ring whose bolometric luminosity, radius, and total mass are L_{SB} , R_{SB} , and M_{SB} , respectively. (Even if the starburst regions are localized, the radiation fields could be equivalent to those of a ringlike source owing to the short rotation timescale; see also Paper I). We also include an AGN itself, in which the bolometric luminosity is L_{AGN} , and we simply

assume an energy spectrum of $L_{\nu}^{\text{AGN}} \propto \nu^{-1}$ between 0.01 and 100 keV (Blandford et al. 1990). To calculate the bolometric luminosity and the energy spectrum of the starburst ring, we assume the initial mass function (IMF) to be of Salpeter-type,

$$\phi \propto (m_*/M_{\odot})^{-1.35}, \quad (1)$$

and the star formation rate (SFR) in the starburst regions to be

$$\text{SFR} \propto \exp\left(-\frac{t_{\text{SB}}}{10^7 \text{ yr}}\right), \quad (2)$$

where t_{SB} is the elapsed time after the initial starburst. The total luminosity is regulated by the mass-luminosity relation $(l_*/L_{\odot}) = (m_*/M_{\odot})^{3.7}$ and the mass-age relation $\tau = 1.1 \times 10^{10} \text{ yr } (m_*/M_{\odot})^{-2.7}$, where m_* and l_* are the stellar mass and stellar luminosity, respectively. Here we consider the 2–40 M_{\odot} mass range in the IMF since several observations indicate that the IMF is deficient in low-mass stars with a cutoff of about 2 M_{\odot} , and the upper mass limit is inferred to be around 40 M_{\odot} (Doyon, Puxley, & Joseph 1992; Charlot et al. 1993; Doane & Mathews 1993; Hill et al. 1994; Brandl et al. 1996). In addition, we employ the mass-temperature relation $(T_*/T_{\odot}) = (m_*/M_{\odot})^{0.575}$, and the energy spectrum of the star is assumed to be the blackbody spectrum with the effective temperature T_* . We neglect the radiation from the supernovae because the long-term averaged luminosity of supernovae is less than 10% of the total stellar luminosity of the ring, as shown in Paper I. As a result, the bolometric luminosity of the starburst ring is in proportion to the total mass and decreases with time.

As for the gravitational fields, we should consider the galactic bulge, the central black hole, and the starburst ring, but the gravitational fields in circumnuclear regions suffer from some uncertainty. Recent observations provide significant information that allows us to model the gravitational fields in circumnuclear regions. For instance, the stellar rotation velocity in the Circinus galaxy (the closest Seyfert 2 galaxy) shows that the mass distributions in circumnuclear regions are not concentrated into a pointlike object but extended to a few hundred parsecs (Maiolino et al. 1998a). Therefore, we also consider such an inner bulgelike component. We assume the galactic bulge to be a uniform sphere whose mass and radius are M_{GB} and R_{GB} , respectively, the inner bulge also to be a uniform sphere whose mass and radius are M_{IB} and R_{IB} , respectively, and the mass of the black hole to be M_{BH} .

The observations of *IRAS* galaxies by Scoville et al. (1991) show that the central regions within kiloparsecs possess the mass of $\lesssim 10^{10} M_{\odot}$. This is comparable to a typical mass of the galactic bulge. A rotation velocity of a starburst ring also implies that the dynamical mass within a few hundred parsecs is several times $10^9 M_{\odot}$ (Elmouttie et al. 1998), which provides an estimation of the mass of the inner bulge. In addition, Maiolino et al. (1998a) estimated an upper limit of a putative black hole as several times $10^6 M_{\odot}$. (We tentatively assume the black hole mass to be $10^7 M_{\odot}$, but the overall results are not changed much even if one assumes $M_{\text{BH}} = 10^6$ or $10^8 M_{\odot}$.) By taking these observational data into account, we adopt the mass ratio of $M_{\text{GB}}:M_{\text{IB}}:M_{\text{BH}} = 1:0.1:10^{-3}$. On the other hand, the mass of the starburst ring M_{SB} is supposed to be between 10^7 and $10^{10} M_{\odot}$. Also, a star-forming ring is observed around a few hundred parsecs in some galaxies (Marconi et al. 1994;

Elmouttie et al. 1998). Hence, here we assume a starburst ring at a radius of 200 pc. For the size ratios, we employ $R_{\text{GB}}:R_{\text{SB}}:R_{\text{IB}} = 5:1:0.5$.

3. STRUCTURE OF THE RADIATIVELY SUPPORTED OBSCURING WALL

The equilibrium configuration of dusty gas is nearly spherically symmetric, as is shown in § 4. Thus, first we investigate the structure of a radiatively supported gas wall inside the starburst ring under an approximation of local spherical symmetry. For this purpose, we assume the gravity of the starburst ring to be constant at the part of the wall of interest. Also, the radiation force of the starburst ring is assumed to be a function solely of the optical depth measured from the outer surface of the wall. (Rigidly speaking, both assumptions are verified only when the wall is geometrically thin and located on the equatorial plane.) Under these assumptions, we solve the one-dimensional radiation-hydrostatic equation, coupled with the ionization and thermal processes.

The radiation-hydrostatic equation is given by

$$-\frac{GM_l}{l^2} - \frac{1}{\rho_g} \frac{dP_g}{dl} + \int \frac{\chi_v}{c} \frac{L_v^{\text{AGN}} e^{-\tau_v}}{4\pi l^2} dv + f_{\text{grav}}^{\text{SB}} - \int \frac{\chi_v}{c} F_v^{\text{SB}} e^{-(\tau_v^{\text{total}} - \tau_v)} dv = 0, \quad (3)$$

where l is the radius, M_l is the total mass within the radius l , ρ_g is the gas density, P_g is the gas pressure, χ_v is the mass extinction coefficient of dusty gas, τ_v is the optical depth of the wall measured from the center, τ_v^{total} is the total optical depth of the wall, and $f_{\text{grav}}^{\text{SB}}$ and F_v^{SB} are the gravity and the radiation flux of the starburst ring, respectively. It is noted that $f_{\text{grav}}^{\text{SB}}$ and F_v^{SB} provide nonspherical components in real situations. The effects of the nonsphericity are taken into consideration by evaluating these quantities using two-dimensional axisymmetric calculations.

Recent observations report the existence of a large amount of dust, molecular gas, and metals in QSOs (Barvainis et al. 1992; Ohta et al. 1996; Omont et al. 1996; Dietrich & Wilhelm-Erkens 2000). Therefore, we suppose the dust-to-gas mass ratio to be 0.03, which is 3 times as large as that observed in the solar neighborhood. Since the mass density of dust and Thomson scattering is negligible, the extinction is given by $\chi_v = (n_{\text{H}} \chi_{\text{H I}} \sigma_{\text{H I}}^{\text{H I}} + \alpha_d^{\text{d}}) / \rho_g$. Here n_{H} is the number density of hydrogen nuclei, $\chi_{\text{H I}}$ is the fraction of neutral hydrogen, $\sigma_{\text{H I}}^{\text{H I}}$ is the photoionization cross section, and α_d^{d} is the absorption coefficient of dust. For the dust model, we employ the grain size distribution as $n_d(a_d) \propto a_d^{-3.5}$ in a range of 0.01–1 μm (Mathis, Rumpl, & Nordsieck 1977) and an absorption cross section, $\pi a_d^2 \min[1, (\lambda/2\pi a_d)^{-2}]$, where a_d is the grain radius and the density of solid material within a grain is assumed to be 1.0 g cm^{-3} .

The equation of the ionization balance is

$$\Gamma^\gamma \chi_{\text{H I}} + \Gamma^{\text{ci}} n_{\text{H}} \chi_{\text{H I}} (1 - \chi_{\text{H I}}) = \alpha_{\text{rec}} n_{\text{H}} (1 - \chi_{\text{H I}})^2, \quad (4)$$

where Γ^γ is the photoionization rate, Γ^{ci} is the collisional ionization rate, and α_{rec} is the recombination coefficient. Γ^γ is given by

$$\Gamma^\gamma = \int_{\nu_{\text{L}}} \sigma_{\text{H I}}^{\text{H I}} \left(\frac{L_v^{\text{AGN}} e^{-\tau_v}}{4\pi l^2} + F_v^{\text{SB}} e^{-(\tau_v^{\text{total}} - \tau_v)} \right) \frac{1}{h\nu} dv, \quad (5)$$

where ν_{L} is the Lyman limit frequency and Γ^{ci} is $1.19 \times 10^{-10} T_g^{1/2} \exp(-1.58 \times 10^5/T_g)$ (Sherman 1979). If a free electron recombines directly to the ground state of hydrogen, the emitted photon has enough energy to cause further photoionization. Since a part of the recombination photons is absorbed by the dust grain, the value α_{rec} is given by

$$\alpha_{\text{rec}} = \alpha_A - (\alpha_A - \alpha_B) n_{\text{H}} \chi_{\text{H I}} \sigma_{\text{H I}}^{\text{H I}} / \rho_g \chi_{\text{H I}},$$

where the total recombination coefficient α_A is well fitted by

$$\alpha_A = 2.1 \times 10^{-13} (T_g/10^4 \text{ K})^{-1/2} \phi(16T_g/10^4 \text{ K}),$$

with $\phi(y) = 0.5(1.7 + \ln y + 1/6y)$ for $y \geq 0.5$ or $y(-0.3 - 1.2 \ln y) + y^2(0.5 - \ln y)$ for $y < 0.5$ (Sherman 1979), and the recombination coefficient to all excited levels of hydrogen α_B is approximately related to α_A as $\alpha_B = \alpha_A \exp[-0.487(T_g/10^4 \text{ K})^{1/5}]$, where T_g is the gas temperature.

The equation for the energy balance of the gas is given by

$$\mathcal{H}_g^\gamma = \mathcal{L}_g^{\text{rec}} + \mathcal{L}_g^{\text{ff}} + \mathcal{L}_g^{\text{ci}} + \mathcal{L}_g^{\text{ce}} + \mathcal{L}_g^{\text{Z}} + \mathcal{L}_g^{\text{gd}}, \quad (6)$$

where \mathcal{H}_g^γ is the heating rate of the gas due to direct radiation of the starburst ring as well as the AGN, and $\mathcal{L}_g^{\text{rec}}$, $\mathcal{L}_g^{\text{ff}}$, $\mathcal{L}_g^{\text{ci}}$, $\mathcal{L}_g^{\text{ce}}$, \mathcal{L}_g^{Z} , and $\mathcal{L}_g^{\text{gd}}$ are the cooling rates for gas through radiative recombination, free-free emission, collisional ionization, collisional excitation, emission for metal, and collision with dust, respectively. \mathcal{H}_g^γ is given by

$$\mathcal{H}_g^\gamma = \int_{\nu_{\text{L}}} \chi_{\text{H I}} \sigma_{\text{H I}}^{\text{H I}} \left(\frac{L_v^{\text{AGN}} e^{-\tau_v}}{4\pi l^2} + F_v^{\text{SB}} e^{-(\tau_v^{\text{total}} - \tau_v)} \right) \left(1 - \frac{\nu_{\text{L}}}{\nu} \right) dv, \quad (7)$$

where we neglect the energy transfer by the Compton scattering because the timescale is estimated to be $\sim 10^9$ yr, which is much longer than the typical lifetime of AGNs, $\sim 10^8$ yr, in the circumnuclear regions of greater than several times 10 pc even in the case of very luminous AGNs with $\sim 10^{13} L_\odot$. $\mathcal{L}_g^{\text{rec}}$, $\mathcal{L}_g^{\text{ff}}$, $\mathcal{L}_g^{\text{ci}}$, and $\mathcal{L}_g^{\text{ce}}$ are represented by

$$\begin{aligned} \mathcal{L}_g^{\text{rec}} &= 3kT_g \alpha_{\text{rec}} n_{\text{H}} (1 - \chi_{\text{H I}})^2 / 2, \\ \mathcal{L}_g^{\text{ff}} &= 1.42 \times 10^{-27} T_g^{1/2} n_{\text{H}} (1 - \chi_{\text{H I}})^2, \\ \mathcal{L}_g^{\text{ci}} &= \Gamma^{\text{ci}} h\nu_{\text{L}} n_{\text{H}} \chi_{\text{H I}} (1 - \chi_{\text{H I}}), \\ \mathcal{L}_g^{\text{ce}} &= 7.5 \times 10^{-19} \exp(-1.18 \times 10^5/T_g) \\ &\quad \times n_{\text{H}} \chi_{\text{H I}} (1 - \chi_{\text{H I}}) \end{aligned}$$

(Black 1981), and

$$\mathcal{L}_g^{\text{Z}} = 4 \times 10^{-28} T_g^{1/2} n_{\text{H}}$$

for $10^2 \text{ K} < T_g < 10^4 \text{ K}$ or

$$\mathcal{L}_g^{\text{Z}} = 10^{-(120Z + 22.1)} T_g^{30Z} n_{\text{H}} - 10^{-22.1} n_{\text{H}}$$

for $10^4 \text{ K} < T_g < 10^5 \text{ K}$ (Theis, Burkert, & Hensler 1992), where Z is the metal abundance. Here the metal abundance is assumed to be 3 Z_\odot , which is consistent with the supposed dust-to-gas mass ratio of 0.03. Assuming the collisional equilibrium of a charge on a grain, we can estimate

$$\mathcal{L}_g^{\text{gd}} = \int n_d \pi a_d^2 da_d (7 - 6\chi_{\text{H I}}) (8kT_g/\pi m_p)^{1/2} (2kT_g - 2kT_d),$$

where m_p is the proton mass and T_d is the dust temperature. As for the energy balance for dust, the emission from gas is assumed to be absorbed by dust almost on the spot. Then the energy equation for dust is

$$\mathcal{H}_d^\gamma + \mathcal{L}_g^{\text{rec}} + \mathcal{L}_g^{\text{ff}} + \mathcal{L}_g^{\text{ce}} + \mathcal{L}_g^{\text{Z}} + \mathcal{L}_g^{\text{gd}} = \mathcal{L}_d^\gamma, \quad (8)$$

where \mathcal{H}_d^γ and $\mathcal{L}_g^{\text{rec}}$ are the heating rates for dust due to the direct radiation from a starburst ring as well as an AGN and to the recombination photons from hydrogen, respectively, and \mathcal{L}_d^γ is the cooling by dust emission. (This assumption is justified by the fact that a resultant gas wall is optically thick because of dust opacity.) \mathcal{H}_d^γ is given by

$$\mathcal{H}_d^\gamma = \frac{1}{n_H} \int \alpha_v^d \left(\frac{L_v^{\text{AGN}} e^{-\tau_v}}{4\pi l^2} + F_v^{\text{SB}} e^{-(\tau_v^{\text{total}} - \tau_v)} \right) dv, \quad (9)$$

$\mathcal{L}_g^{\text{rec}}$ is written as

$$\mathcal{L}_g^{\text{rec}} = (3kT_g/2 + hv_L) \alpha_{\text{rec}} n_H (1 - \chi_H)^2,$$

and \mathcal{L}_d^γ is presented as

$$\mathcal{L}_d^\gamma = (\sigma \alpha_{v_0}^d / \pi n_H) [\Gamma(6)\zeta(6)/\Gamma(4)\zeta(4)] (k/hv_0)^2 T_d^6,$$

where Γ and ζ are the gamma function and Riemann's function, respectively (Nakamoto & Nakagawa 1994). We note that dust is primarily heated by the direct radiation so that the dust temperature is not affected heavily even if the heating by the gas emission is dismissed. Moreover, since the absorption cross section against IR radiation reemitted from dust is much smaller than that against optical or UV radiation, we suppose that dust grains work as pure absorbers.

The above equations and the equation of state for ideal gas are solved to give the gas density, the gas temperature, the fraction of neutral hydrogen, and the dust temperature as functions of radii. The resultant profile of the hydrogen number density and A_V measured from the center are shown in Figure 1. Here $L_{\text{AGN}} = 10^{10} L_\odot$, $M_{\text{SB}} = 10^9 M_\odot$, and $L_{\text{SB}} = 8.3 \times 10^{10} L_\odot$ ($t_{\text{SB}} = 3 \times 10^7$ yr) are assumed. As seen in this figure, there forms an optically thick wall in

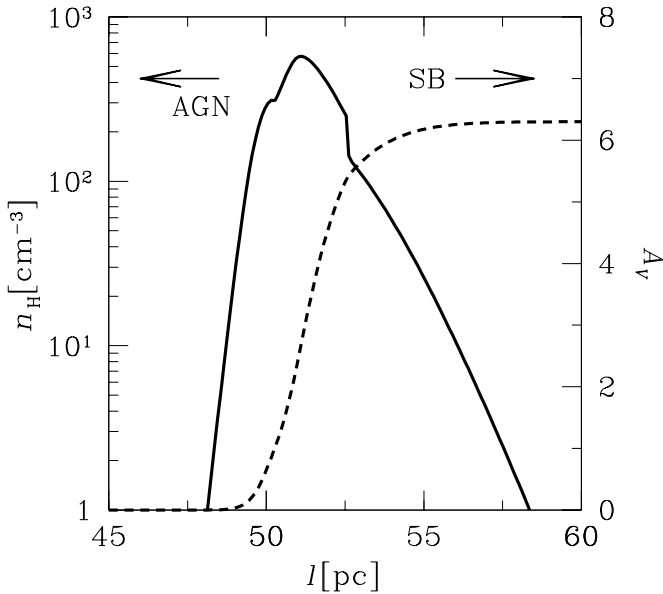


FIG. 1.—Profile of the hydrogen number density and the visual extinction A_V measured from the center as functions of radii l . Here $L_{\text{AGN}} = 10^{10} L_\odot$, $M_{\text{SB}} = 10^9 M_\odot$, and $L_{\text{SB}} = 8.3 \times 10^{10} L_\odot$ ($t_{\text{SB}} = 3 \times 10^7$ yr) are assumed. The AGN is located at the center, $l = 0$, and the size of the starburst ring is assumed to be 200 pc. The interior and exterior surfaces of the wall are irradiated by the radiation from the AGN and the starburst ring, respectively. The density gradient is very steep since the wall is compressed because of the strong radiation force of the starburst ring as well as the AGN. The effective thickness of the wall is less than 10% of its radial extension. This figure shows that a geometrically thin, optically thick wall forms.

which the inner surface is pushed outward by the radiation force of the AGN against the gravity of the inner bulge and the radiation force of the starburst shoves the wall inward. The optical depth (A_V) is basically determined by the ratio of the net radiation force to the total gravity if both the AGN and starburst are super-Eddington luminous to M_I and to M_{SB} , respectively. The density profile of the wall has a peak at ~ 50 pc, and the density gradients on both sides of the peak are very steep. Then the geometrical thickness of the wall is basically determined by the ratio of the square of the sound speed to the total radiation force. The gas temperature is around 10^4 K because of the photoheating. As a result, the effective thickness of the wall is less than 10% of its radial extension. Hence, it is concluded that a radiatively supported wall can be optically thick and geometrically thin. If the starburst is more luminous, the wall would be thinner because the density gradient would be steeper owing to the radiation force. On the other hand, if the mass of the starburst ring is less than $10^9 M_\odot$, the density profile would be roughly the same since the force fields are mainly determined from the AGN and the inner bulge. In this analysis it has turned out that the radiation force from the AGN as well as the starburst is exerted mainly on dust. Therefore, for the mass extinction of the dusty gas, we take only the dust opacity into account in the two-dimensional calculations below.

Although we have considered the structure of a gas wall inside the starburst ring, the structure of an outer wall beyond the starburst ring can be understood by a similar argument. If an outer wall forms at several hundred parsecs, the photoheating does not work effectively to raise the temperature $\sim 10^4$ K, but it does raise the temperature $\sim 10^2$ K. Then the thickness of the wall is much thinner than the inner wall. As for the optical depth (A_V), it is determined basically by the ratio of the radiation force to the total gravity for super-Eddington luminosity, and therefore could be $A_V \gg 1$ mag.

4. CONFIGURATION OF THE OBSCURING WALLS

In this section, we examine the equilibrium configuration of a gas wall and the stability in two-dimensional axisymmetric space. We assume the wall to be geometrically thin, as determined in the previous section. Under that assumption, taking the effects of the optical depth into account, we calculate the radiation force and the gravity that are exerted on a dusty wall. The radiative flux force of the starburst ring is given by

$$f_{\text{SB}}^i = \int \frac{\bar{\chi}_{\text{SB}}}{c} \frac{\rho_{\text{SB}}}{4\pi l_{\text{SB}}^2} \frac{1 - \exp(-\tau_{\text{SB}}/\cos \theta_{\text{SB}})}{\tau_{\text{SB}}/\cos \theta_{\text{SB}}} n^i dV, \quad (10)$$

at a point (r, z) in cylindrical coordinates, where i denotes r or z , $\bar{\chi}_{\text{SB}}$ is the flux mean mass extinction coefficient averaged over the starburst radiation, τ_{SB} is the total optical depth of the wall that is estimated using $\bar{\chi}_{\text{SB}}$, ρ_{SB} is the luminosity density in the starburst ring, l_{SB} is the distance from (r, z) to a volume element dV of the ring, θ_{SB} is the viewing angle from this element, and n^i is the directional cosine. Similarly, the radiative flux force of the AGN is

$$f_{\text{AGN}}^i = \frac{\bar{\chi}_{\text{AGN}}}{c} \frac{L_{\text{AGN}}}{4\pi l^2} \frac{1 - \exp(-\tau_{\text{AGN}}/\cos \theta_{\text{AGN}})}{\tau_{\text{AGN}}/\cos \theta_{\text{AGN}}} \frac{i}{l} \quad (11)$$

at the same point, where $\bar{\chi}_{\text{AGN}}$ is the flux mean mass extinc-

tion averaged over the AGN radiation, l is the distance, θ_{AGN} is the viewing angle from the center, and τ_{AGN} is the total optical depth, which is estimated using $\bar{\chi}_{\text{AGN}}$. Using equations (10) and (11), the equilibrium between the radiation force and the gravity is determined with

$$-\frac{d\Phi}{dz} = f_{\text{SB}}^z + f_{\text{AGN}}^z + f_{\text{grav}}^z = 0, \quad (12)$$

in the vertical directions (z -directions) and

$$-\frac{d\Phi}{dr} = \frac{j^2}{r^3} + f_{\text{SB}}^r + f_{\text{AGN}}^r + f_{\text{grav}}^r = 0, \quad (13)$$

in the radial directions (r -directions), where Φ is the effective potential, j is the specific angular momentum of the dusty gas, and f_{grav}^i is the gravitational force. Furthermore, stable configuration should satisfy the conditions

$$\frac{d^2\Phi}{dz^2} > 0, \quad (14)$$

$$\frac{d^2\Phi}{dr^2} > 0. \quad (15)$$

4.1. Inner Obscuring Wall

First, we consider the formation of a dusty wall inside the starburst ring. The wall is irradiated outward by the AGN and inward by the starburst ring. In Figure 2, the resultant equilibrium branches are shown in the r - z space for $A_V = 3, 5, \text{ and } 7$ mag. Here $L_{\text{AGN}} = 10^{10} L_{\odot}$, $M_{\text{SB}} = 10^9 M_{\odot}$, and $L_{\text{SB}} = 8.3 \times 10^{10} L_{\odot}$ ($t_{\text{SB}} = 3 \times 10^7 \text{ yr}$) are assumed. On each curve, the conditions for stable equilibrium in the ver-

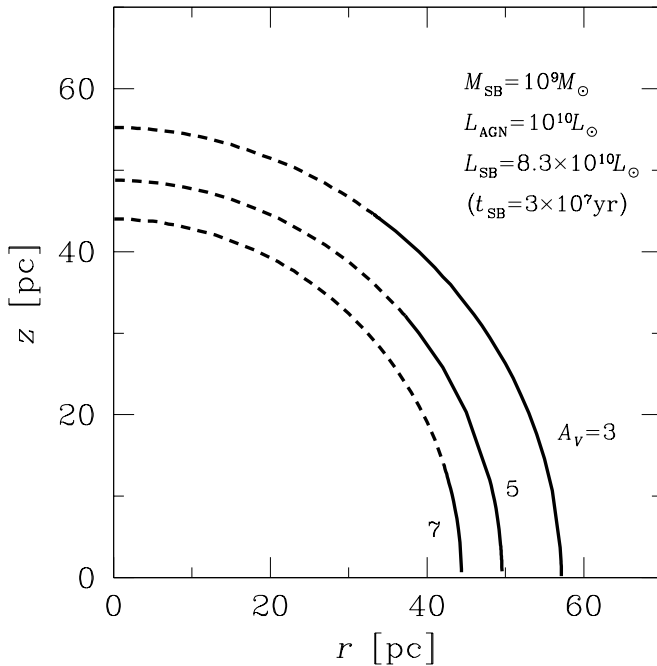


FIG. 2.—Equilibrium configuration of inner walls in r - z space for $A_V = 3, 5, \text{ and } 7$. Here $L_{\text{AGN}} = 10^{10} L_{\odot}$, $M_{\text{SB}} = 10^9 M_{\odot}$, and $L_{\text{SB}} = 8.3 \times 10^{10} L_{\odot}$ ($t_{\text{SB}} = 3 \times 10^7 \text{ yr}$) are assumed. The solid curves represent the stable branches, while the dashed curves are radially nonequilibrium branches. The solid curves show the final configuration of stable inner walls. Since the effective radiation force of the ring is weakened in the vicinity of the rotation axis in the case of the inner wall because of a large viewing angle, an opening forms, and it is shown by a dashed curve.

tical directions (eqs. [12] and [14]) are satisfied. However, the dashed curves do not satisfy the force balance (eq. [13]) in the radial directions, so that the dusty gas is likely to be swung away around the curves because of centrifugal force. As a result, it is found that the solid curves are the stable equilibrium branches in both the vertical and radial directions, which provides the final configuration of the inner obscuring wall. It is noted that the starburst ring plays an important role in the force balance and the stability of the wall. The AGN as well as the bulge components provide only spherically symmetric forces, whereas the radiation force and the gravity of the starburst ring are not spherically symmetric. Therefore, on the tangential plane, the azimuthal component of centrifugal force can balance only with that of the radiation force of the ring (see Fig. 3). To realize this situation, the starburst luminosity is required to be super-Eddington, $L_{\text{SB}} > 4\pi c G M_{\text{SB}} / \bar{\chi}_{\text{SB}}$. Since the effective radiation force of the starburst ring is weakened for a large viewing angle θ_{SB} , the radial balance breaks down in the vicinity of the rotation axis (z -axis). An opening grows as the optical depth (A_V) increases because of the dilution of the effective radiation force of the ring (see eq. [10]). In order for a stable inner wall to enshroud the nuclear regions with a large covering factor (opening angle $< 90^\circ$), A_V is constrained from above as

$$A_V \lesssim \frac{\chi_V L_{\text{SB}}}{4\pi c G M_{\text{SB}}}, \quad (16)$$

where χ_V is the mass extinction at the V band. On the other hand, the radiation force of a very luminous AGN could blow the dusty gas away from the inner bulge regions if the optical depth is not enough to dilute the radiation force.

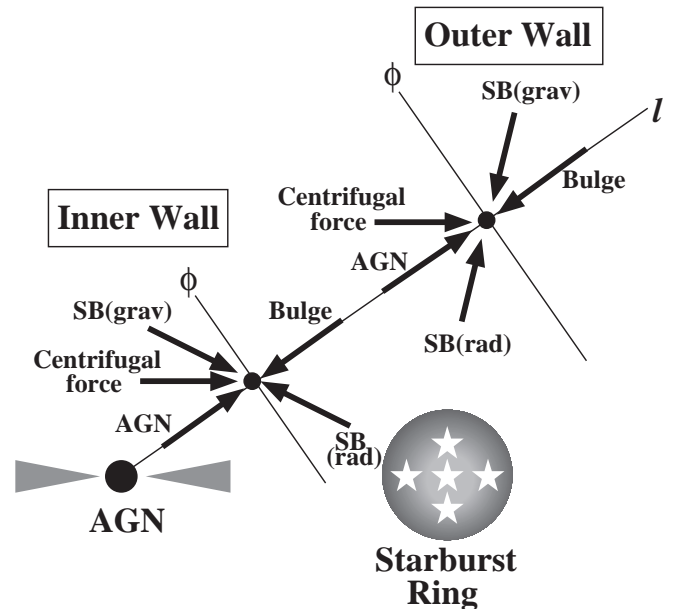


FIG. 3.—Schematic edge-on sketch showing the forces exerted on the inner wall as well as the outer wall. Arrows represent the orientations of the forces, although the lengths of the arrows do not correspond to the strength of the forces. As a result of numerical calculation, it is found that the starburst ring provides nonspherical radiation force and gravity, whereas the forces by the AGN as well as the bulge components are spherically symmetric. Hence, the walls form if the azimuthal (Φ) component of radiation force of the starburst ring balances with that of the total force of the gravity by the ring and the centrifugal force.

This provides a lower bound of A_V as

$$A_V > \frac{\chi_V L_{\text{AGN}}}{4\pi c G (M_{\text{IB}} + M_{\text{BH}})}. \quad (17)$$

Because of the time dependence of starburst luminosity, the upper bound of A_V given by equation (16) is a decreasing function of time. For a given model, the allowed range of A_V of the inner wall is presented in Figure 4 as a function of time t_{SB} . In the shaded regions, no stable equilibrium branches with a large covering factor exist, and in the hatched regions the radiation force of the AGN blows out the dusty gas. If the upper bound in equation (16) is smaller than the lower bound in equation (17), there is no allowed value for A_V . That is to say, no inner wall forms regardless of t_{SB} if

$$L_{\text{AGN}} > (M_{\text{IB}} + M_{\text{BH}}) \frac{L_{\text{SB}}}{M_{\text{SB}}}. \quad (18)$$

4.2. Outer Obscuring Wall

Next, we investigate the formation of an outer wall with the radial extension of $\geq R_{\text{SB}}$. In Figure 5, the resultant equilibrium branches of the outer wall are shown in the r - z plane. As shown in this figure, a nearly spherical wall forms. In this case, the starburst ring as well as the AGN irradiate the inside of the wall. Therefore, the radiation force of the starburst ring is exerted outward on the dusty wall, although the inner wall is pushed inward by the starburst radiation, but it has been found by the present analyses that the radial equilibrium and the stable condition for the outer wall formation are again given by equation (16) for a wide range of parameters. It is also required that the starburst ring be super-Eddington luminous. This can also be under-

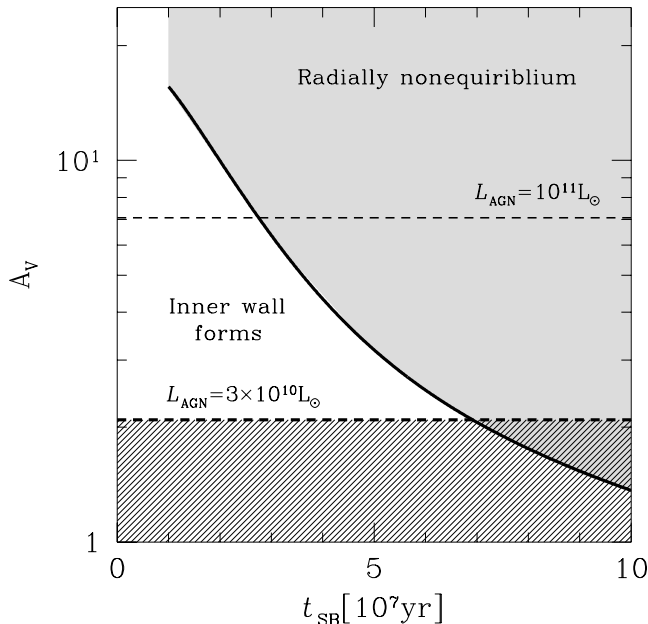


FIG. 4.—Range of A_V allowed for the inner wall formation. In the shaded area, A_V does not satisfy eq. (16), so that the greater part of the wall is out of radial equilibrium. Also, the dusty gas is blown away because of the strong radiation force of the AGN in the hatched area in the case of $L_{\text{AGN}} = 3 \times 10^{10} L_{\odot}$.

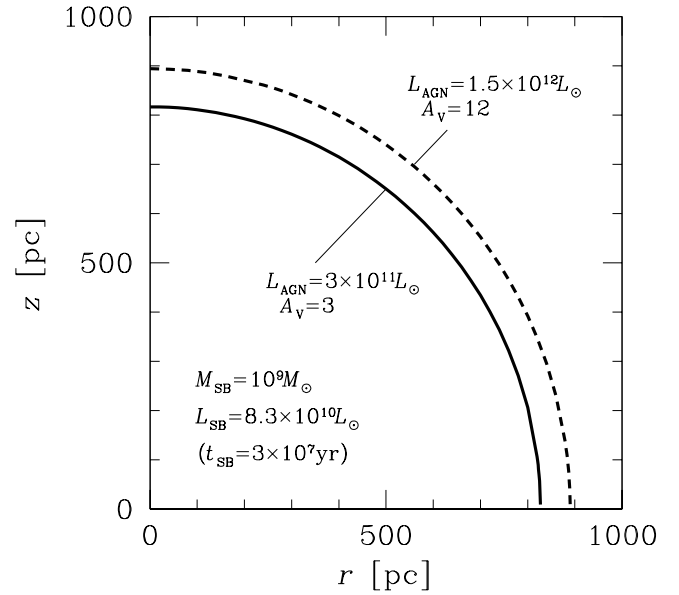


FIG. 5.—Equilibrium configuration of an outer wall beyond the starburst regions in r - z space for two cases of the AGN luminosity, say, $L_{\text{AGN}} = 3 \times 10^{11}$ and $1.5 \times 10^{12} L_{\odot}$. Here $M_{\text{SB}} = 10^9 M_{\odot}$ and $L_{\text{SB}} = 8.3 \times 10^{10} L_{\odot}$ are assumed. The solid curve represents stable branches, while the dashed curve is the radially nonequilibrium branches. The outer wall is roughly of spherical shape and covers a wide solid angle whenever it forms.

stood by the argument of force balance in the azimuthal directions at a point on the wall. The azimuthal component of the centrifugal force can be balanced only by the force of the starburst ring because only the starburst ring provides a spherical force (see Fig. 3). The upper value of the allowed A_V decreases again with time as the starburst becomes dimmer. As a prerequisite condition for the formation of the wall, $(\bar{\chi}_{\text{AGN}} L_{\text{AGN}} + \bar{\chi}_{\text{SB}} L_{\text{SB}})/4\pi c G (M_{\text{SB}} + M_{\text{IB}} + M_{\text{BH}}) > 1$ is required; otherwise, the dusty gas is not held at the regions of greater than R_{IB} even in the case of an optically thin wall. Since the radiation force is diluted by the optical depth of the wall, the upper bound of A_V is provided as

$$A_V < \frac{\chi_V (L_{\text{AGN}} + L_{\text{SB}})}{4\pi c G (M_{\text{SB}} + M_{\text{IB}} + M_{\text{BH}})}, \quad (19)$$

for the sustainment of the dusty gas. On the other hand, the lower bound of A_V is estimated by

$$A_V > \frac{\chi_V (L_{\text{AGN}} + L_{\text{SB}})}{4\pi c G (M_{\text{GB}} + M_{\text{SB}} + M_{\text{IB}} + M_{\text{BH}})}, \quad (20)$$

since the radiation force would blow out the dusty gas in most regions if the A_V of the wall is smaller than this value. Comparing this lower limit to equation (16), we find that no outer wall forms if the AGN luminosity satisfies the inequality as

$$L_{\text{AGN}} > (M_{\text{GB}} + M_{\text{IB}} + M_{\text{BH}}) \frac{L_{\text{SB}}}{M_{\text{SB}}}. \quad (21)$$

It is noted that this condition involves the prohibition equation (18) for an inner wall. A_V is limited from above as

$$A_V < \min \left[\frac{\chi_V L_{\text{SB}}}{4\pi c G M_{\text{SB}}}, \frac{\chi_V (L_{\text{AGN}} + L_{\text{SB}})}{4\pi c G (M_{\text{SB}} + M_{\text{IB}} + M_{\text{BH}})} \right]. \quad (22)$$

5. IMPLICATIONS FOR THE STARBURST-AGN CONNECTION

From the viewpoint of the formation of radiatively supported obscuring walls, we discuss the connection between the AGN type and the starburst events. Based on the conditions of equations (18) and (21), in Figure 6 the prediction for the wall formation is summarized in a diagram of L_{AGN} versus $L_{\text{SB}}/M_{\text{SB},9}$, where $M_{\text{SB},9}$ is the mass of a starburst in units of $10^9 M_{\odot}$. An outer wall forms below the solid line, and an inner wall as well as an outer wall form below the dashed line. A vertical dot-dashed line shows the boundary for the formation of the walls. The possible values of A_V are also shown by the thin dot-dashed lines. Here it is stressed that the possible A_V is practically determined by equation (22) for the outer wall. However, if the mass supply to an altitude of several times 100 pc of a superbubble driven by a circumnuclear starburst is insufficient, no outer wall of $A_V \gtrsim$ several magnitudes might form (see § 6). The figure shows that for a luminous starburst and a relatively faint AGN, both inner and outer walls are built up, and the nucleus could be obscured with the total extinction of $A_V \sim 10$ mag. Then the nucleus is likely to be identified as a type 2 AGN (Seyfert 2 galaxies). Also, the outer wall may be consistent with the recently observed obscuring material extending up to ≥ 100 pc around the nuclei (Rudy et al.

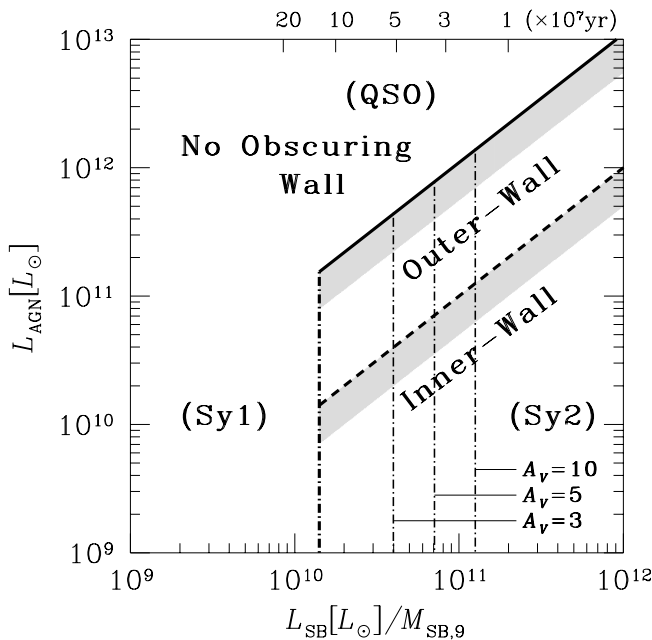


FIG. 6.—Conditions for the formation of obscuring walls in a diagram of the AGN luminosity L_{AGN} vs. the starburst luminosity L_{SB} , where the starburst luminosity is divided by the mass of the starburst in units of $10^9 M_{\odot}$. An outer wall forms below the solid line and an inner wall as well as an outer wall form below the dashed line. A vertical dot-dashed line gives the boundary for the formation of the walls based on the condition that the starburst is super-Eddington luminous, and the specific values of A_V are also shown by thin dot-dashed lines. The figure shows that for a luminous starburst and a relatively faint AGN, the nucleus is enshrouded by double walls with the total extinction of $A_V > 10$ mag, and therefore it is likely to be identified as a type 2 AGN (Seyfert 2 galaxy). If a starburst is intrinsically faint or becomes dimmer owing to the stellar evolution, neither wall forms, and the nucleus is observed as a type 1 AGN (Seyfert 1 galaxy). The age of the starburst based on the present stellar evolution model is shown in the upper abscissa. Furthermore, if the AGN is much more luminous, the wall formation is prohibited regardless of the starburst luminosity (QSO).

1988; Miller et al. 1991; Goodrich 1995; McLeod & Rieke 1995a; Maiolino et al. 1995; Maiolino & Rieke 1995; Malkan et al. 1998).

By X-ray observations, the A_V of most Seyfert 2 nuclei is estimated to be greater than 10 and sometimes greater than 100 mag. Such a difference between the values of A_V estimated by the X-ray observations and the values of A_V assessed by the IR or optical observations might be due to obscuring matter free from dust located just inside the dust sublimation radius of subparsec. The structure and formation mechanism of obscuring material in subparsec regions is debatable, but it is beyond the scope of this paper.

If a starburst is intrinsically faint, neither an outer wall nor an inner one is expected to form. Then the nucleus could be observed as a type 1 AGN (Seyfert 1 galaxy). These results provide a physical explanation for the putative correlation between AGN type and host properties whereby Seyfert 2 galaxies are more frequently associated with circumnuclear starbursts than type 1 galaxies. Also, the moderate extinction by the walls may lead to intermediate types of AGNs, that is, type 1.9, 1.8, 1.5, or 1.2 according to the decrease of the extinction.

In addition, we have come to a significant conclusion that much higher AGN activity since equation (21) would preclude either wall from forming. Then the nucleus tends to be identified as type 1 regardless of the starburst luminosity. This result may be closely related to the fact that QSOs are mostly observed as type 1 regardless of star-forming activity in the host galaxies.

6. AGN EVOLUTION

In the previous section, it is shown that the obscuring walls form in the case of the luminous starburst and the relatively faint AGN. It implies that the obscuration of the AGN is time-dependent since the bolometric luminosity of the starburst ring decreases with time because of stellar evolution. In this section, we discuss the evolution of the AGN type predicted by this picture. The schematic view of the evolution of the circumnuclear structure is shown in Figure 7.

In an early evolutionary stage, a large amount of dusty gas could be blown out by superbubbles in the circumnuclear starburst regions. Shapiro & Field (1976), Tomisaka & Ikeuchi (1986), and Norman & Ikeuchi (1989) have shown that a superbubble of ~ 1 kpc powered by massive OB associations forms. As an observational example, a superbubble of 1.1 kpc is observed in the region immediately east of the nucleus of nearby Seyfert 2/LINER galaxy NGC 3079 (Veilleux et al. 1994).

Also, if the mass supply rate given by Norman & Ikeuchi (1989) is applied to the case of circumnuclear starbursts of $M_{\text{SB}} \sim 10^9 M_{\odot}$, the rate into the regions of a height of several times 100 pc from the circumnuclear molecular disk due to superbubbles is estimated to be several times $10 M_{\odot} \text{ yr}^{-1}$. In the case of the superbubble of NGC 3079, Duric & Seaquist (1988) and Veilleux et al. (1994) evaluated the mass supply rate to be $\gtrsim 10$ and $\sim 7 M_{\odot} \text{ yr}^{-1}$. As a result, the dusty gas of $\gtrsim 10^8 M_{\odot}$ would be supplied within a typical lifetime of a superbubble ($\sim 10^7$ yr) and composes the obscuring walls in the next stage. However, an outer obscuring wall with $A_V \gtrsim 10$ mag may not form because it requires dusty gas of $\gtrsim 10^8 M_{\odot}$. On the other hand, the required mass for an inner wall is merely $\sim 10^6 M_{\odot}$. The

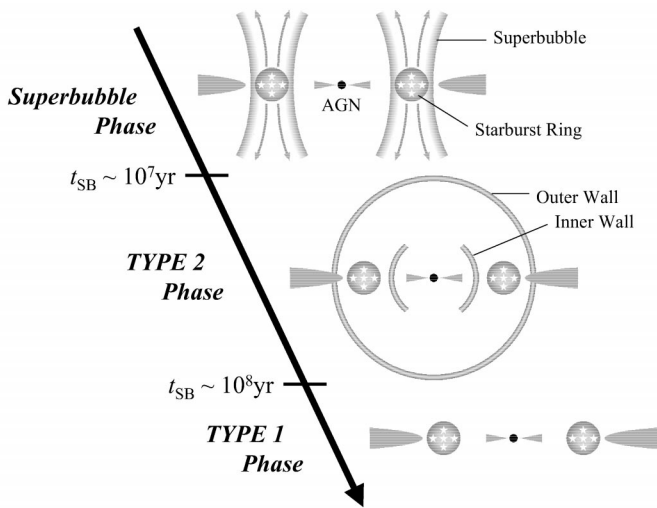


FIG. 7.—Schematic illustration of the evolution of the circumnuclear structure. Within $\sim 10^7$ yr, a large amount of dusty gas is blown away because of superbubbles powered by Type II supernovae in circumnuclear starburst regions. The ejected dusty gas is supported by the radiation force of the AGN as well as the starburst ring and composes the obscuring walls. Then the nucleus is obscured by both walls and tends to be identified as a type 2 AGN (Seyfert 2 galaxy). Based on the present stellar evolution model, the nucleus tends to be observed as a type 2 AGN (Seyfert 2 galaxy) within several times 10^7 yr since the possible A_V decreases with time because of stellar evolution. Finally, the walls disappear, and the nucleus is observed as a type 1 AGN (Seyfert 1 galaxy). Therefore, the AGN is destined to shift from type 2 to type 1 in several times 10^7 yr in this picture. However, QSOs are observed as type 1 AGNs regardless of the age of the starburst because the luminous AGN prevent the formation of the walls.

formation timescales of an inner wall and those of an outer wall are several times 10^5 and several times 10^6 yr, respectively. Both timescales are shorter than the evolutionary timescale of the starburst which is on the order of $\sim 10^7$ yr. Thus, the nucleus is likely to be obscured by the inner wall with $A_V \gtrsim$ several magnitudes as well as the outer wall with $A_V \lesssim$ a few magnitudes, whereas the possible A_V decreases with time because of the stellar evolution in the starburst regions. Based on the present stellar evolution model, the nucleus is heavily obscured and tends to be observed as type 2 AGNs (Seyfert 2 galaxies) within several times 10^7 yr. Also, the inner wall would not be destroyed even if the superbubbles occur in this stage, since the bubble diameter on the equatorial plane is comparable to the scale height of the molecular disk (Schiano 1985; Mac Low & McCray 1988; Tomisaka & Ikeuchi 1988; Mac Low, McCray, & Norman 1989).

In the final stage, the obscuring walls disappear because of the diminution of the bolometric luminosity of the circumnuclear starburst. Then the nucleus would be identified as a type 1 AGN (Seyfert 1 galaxy). To conclude, the AGN type is time-dependent and is destined to shift from type 2 to type 1 in several times 10^7 yr. It is stressed that no obscuring wall forms in the case of the luminous AGN-like QSOs so that the type of the QSO does not vary, and it is observed as type 1 regardless of the age of the starburst.

Here we have assumed that AGN activity and the circumnuclear starbursts are simultaneous events. From an observational point of view, it seems to be reasonable because it is revealed that AGN events are frequently accompanied by starbursts in a variety of data (Scoville et al. 1986; Soifer et al. 1986; Heckman et al. 1989, 1995;

Marconi et al. 1994; Neff et al. 1994; Cid Fernandes & Terlevich 1995; Genzel et al. 1995; Maiolino et al. 1995, 1998a; Oliva et al. 1995; Storchi-Bergmann et al. 1996; Rodriguez-Espinosa, Rudy, & Jones 1987; Elmouttie et al. 1998; Cid Fernandes, Storchi-Bergmann, & Schmitt 1998). In addition, as a physical solution that links the two events, Norman & Scoville (1988) have suggested a model, whereby the interstellar medium that is released by post-main-sequence stars in starburst regions feeds a central black hole. Also, the radiatively driven mass accretion onto a black hole due to the radiation drag, which is proposed by Umemura, Fukue, & Mineshige (1997, 1998), Fukue, Umemura, & Mineshige (1997), and Ohsuga et al. (1999), would link the two events.

In the present analysis, we have assumed the existence of the interstellar gas containing a large amount of dust that is inferred in QSOs (Barvainis et al. 1992; Ohta et al. 1996; Omont et al. 1996; Dietrich & Wilhelm-Erkens 2000). However, the dust grains could be destroyed in shock-heated hot gas, and they could be reproduced in cooled superbubble winds. The dust properties around AGNs are also under debate from an observational point of view. The destruction, formation, and growth of the dust grains would obviously have significant effects not only in the present picture but also in a generic problem of obscuration. Thus, this issue should be considered more carefully in future analysis.

Finally, we discuss the stabilities of the obscuring walls. First of all, the walls are unlikely to be subject to the Rayleigh-Taylor instability. As shown in Figure 1, the density gradient of the inner wall is positive inside the density peak and negative outside the peak. As shown in Figure 3, the acceleration works in the same directions as the density gradient in both sides. Thus, the Rayleigh-Taylor instability does not occur at the inner wall. In the case of the outer wall, the radiation force of the AGN and the starburst ring, which pushes up the wall, is the dominant force at the inner surface, but the dusty gas is attracted by the gravity at the outer surface. As a result, both walls turn out to be stable to the Rayleigh-Taylor mode. However, the walls might be subject to the other instabilities. When the density perturbations occur in the walls, the thick parts of the walls go down by the gravity, whereas the radiation force lifts the less thick parts since the radiation force is ineffective for heavily optically thick parts. Then the walls are likely to have more complicated configurations. Moreover, thermal instabilities might break out because the radiative cooling works at the dense regions effectively, whereas the gas remains as warm as $\sim 10^4$ K in the optically thin regions because of radiative heating. Simultaneously, the self-gravitating instability might grow at the cool and dense parts of the walls. Also, the actual circumnuclear starburst is not perfectly ring-shaped but more or less clumpy and therefore makes nonaxisymmetric radiation fields, although the wheel rotation could smear out nonaxisymmetric effects to some degree (see also Paper I). In addition, the dusty walls are possibly damaged because of the collision of starburst winds or dusty gas expelled from mass-losing stars inside the walls. Consequently, the walls could be distorted and fragment into small pieces. How the gas clouds resulting from the fragmentation obscure the AGN is an interesting issue, but the details will not be clear until radiation-hydrodynamical simulations are performed.

7. CONCLUSIONS

In the present analysis, by taking the optical depth due to dust opacity into consideration, we have analyzed the stable equilibrium configuration of dusty gas in the circumnuclear regions in radiation fields of a starburst and an AGN. It has been found that the radiation pressure of a circumnuclear starburst sustains an inner obscuring wall of several tens of parsecs and an outer obscuring wall of several hundred parsecs. The total extinction of the obscuring walls has turned out to be around 10. Then the nucleus would be identified as type 2. If a starburst is intrinsically faint or becomes dimmer owing to the stellar evolution there, neither an outer wall nor inner one would form. Then the nucleus could be observed as a type 1 AGN (Seyfert 1 galaxy). The results on outer and inner walls share a certain similarity in that the strong radiation force of the AGN prevents the formation of an outer wall as well as an inner wall. These results provide a physical explanation for the correlation between AGN type and host properties, whereby Seyfert 2 galaxies are more frequently associated

with circumnuclear starbursts than type 1 galaxies, whereas QSOs are mostly observed as type 1 AGNs even though vigorous star-forming activities are often observed in the host galaxies. Also, the large-scale outer wall of several hundred parsecs is consistent with the observations of obscuring material extending up to ≥ 100 pc around the nuclei. Finally, this model predicts the time evolution of the AGN type from type 2 to type 1 in several times 10^7 yr as a circumnuclear starburst becomes dimmer because of stellar evolution.

We are grateful to T. Nakamoto and H. Susa for helpful discussion. We also thank the anonymous referee for valuable comments. The calculations were carried out at Center for Computational Physics at the University of Tsukuba. This work is supported in part by Research Fellowships of the Japan Society for the Promotion of Science for Young Scientists 6957 (K. O.) and the Grants-in Aid of the Ministry of Education, Science, Culture, and Sport 09874055 (M. U.).

REFERENCES

- Antonucci, R. 1993, *ARA&A*, 31, 473
 Antonucci, R. R. J. 1984, *ApJ*, 278, 499
 Awaki, H., Koyama, K., Inoue, H., & Halpern, J. P. 1991, *PASJ*, 43, 195
 Bahcall, J. N., Kirhakos, S., Saxe, D. H., & Schneider, D. P. 1997, *ApJ*, 479, 642
 Barth, A. J., Ho, L. C., Filippenko, A. V., & Sargent, W. L. W. 1995, *AJ*, 110, 1009
 Barthel, P. D. 1989, *ApJ*, 336, 601
 Barvainis, R., Antonucci, R., & Coleman, P. 1992, *ApJ*, 399, L19
 Bassani, L., Dadina, M., Maiolino, R., Salvati, M., Risaliti, G., della Ceca, R., Matt, G., & Zamorani, G. 1999, *ApJS*, 121, 473
 Black, J. H. 1981, *MNRAS*, 197, 553
 Blanco, P. R., Ward, M. J., & Wright, G. S. 1990, *MNRAS*, 242, P4
 Blandford, R. D., Netzer, H., Woltjer, L., Courvoisier, T., & Mayor, M. 1990, *Active Galactic Nuclei* (Berlin: Springer)
 Brandl, B., et al. 1996, *ApJ*, 466, 254
 Brotherton, M. S., et al. 1999, *ApJ*, 520, L87
 Buta, R., Purcell, G. B., & Crocker, D. A. 1995, *AJ*, 110, 1588
 Canalizo, G., & Stockton, A. 2000a, *ApJ*, 528, 201
 ———. 2000b, *AJ*, 120, 1750
 Charlot, S., Ferrari, F., Mathews, G. J., & Silk, J. 1993, *ApJ*, 419, L57
 Cid Fernandes, R., Storchi-Bergmann, T., & Schmitt, H. R. 1998, *MNRAS*, 297, 579
 Cid Fernandes, R., & Terlevich, R. 1995, *MNRAS*, 272, 423
 Crawford, C. S., Lehmann, I., Fabian, A. C., Bremer, M. N., & Hasinger, G. 1999, *MNRAS*, 308, 1159
 Dietrich, M., & Wilhelm-Erkens, U. 2000, *A&A*, 354, 17
 Doane, J. S., & Mathews, W. G. 1993, *ApJ*, 419, 573
 Doyon, R., Puxley, P. J., & Joseph, R. D. 1992, *ApJ*, 397, 117
 Duric, N., & Seaquist, E. R. 1988, *ApJ*, 326, 574
 Efstathiou, A., & Rowan-Robinson, M. 1995, *MNRAS*, 273, 649
 Elmouttie, M., Koribalski, B., Gordon, S., Taylor, K., Houghton, S., Lavezzi, T., Haynes, R., & Jones, K. 1998, *MNRAS*, 297, 49
 Forbes, D. A., Norris, R. P., Williger, G. M., & Smith, R. C. 1994, *AJ*, 107, 984
 Fukue, J., Umemura, M., & Mineshige, S. 1997, *PASJ*, 49, 673
 Genzel, R., Weitzel, L., Tacconi-Garman, L. E., Blietz, M., Cameron, M., Krabbe, A., Lutz, D., & Sternberg, A. 1995, *ApJ*, 444, 129
 González Delgado, R. M., Heckman, T., & Leitherer, C. 2001, *ApJ*, 546, 845
 Goodrich, R. W. 1995, *ApJ*, 440, 141
 Goodrich, R. W., Veilleux, S., & Hill, G. J. 1994, *ApJ*, 422, 521
 Heckman, T., Blitz, L., Wilson, A., Armus, L., & Miley, G. 1989, *ApJ*, 342, 735
 Heckman, T., et al. 1995, *ApJ*, 452, 549
 Hill, J. K., Isensee, J. E., Cornett, R. H., Bohlin, R. C., O'Connell, R. W., Roberts, M. S., Smith, A. M., & Stecher, T. P. 1994, *ApJ*, 425, 122
 Hooper, E. J., Impey, C. D., & Foltz, C. B. 1997, *ApJ*, 480, L95
 Hunt, L. K., Malkan, M. A., Salvati, M., Mandolesi, N., Palazzi, E., & Wade, R. 1997, *ApJS*, 108, 229
 Leitherer, C., Vacca, W. D., Conti, P. S., Filippenko, A. V., Robert, C., & Sargent, W. L. W. 1996, *ApJ*, 465, 717
 Kirhakos, S., Bahcall, J. N., Schneider, D. P., & Kristian, J. 1999, *ApJ*, 520, 67
 Krolik, J. H., & Begelman, M. C. 1988, *ApJ*, 329, 702
 Mac Low, M.-M., & McCray, R. 1988, *ApJ*, 324, 776
 Mac Low, M.-M., McCray, R., & Norman, M. L. 1989, *ApJ*, 337, 141
 Maiolino, R., Krabbe, A., Thatte, N., & Genzel, R. 1998a, *ApJ*, 493, 650
 Maiolino, R., & Rieke, G. H. 1995, *ApJ*, 454, 95
 Maiolino, R., Ruiz, M., Rieke, G. H., & Keller, L. D. 1995, *ApJ*, 446, 561
 Maiolino, R., Ruiz, M., Rieke, G. H., & Papadopoulos, P. 1997, *ApJ*, 485, 552
 Maiolino, R., Salvati, M., Bassani, L., Dadina, M., della Ceca, R., Matt, G., Risaliti, G., & Zamorani, G. 1998b, *A&A*, 338, 781
 Malkan, M. A., Gorjian, V., & Tam, R. 1998, *ApJS*, 117, 25
 Manske, V., Henning, Th., & Men'shchikov, A. B. 1998, *A&A*, 331, 52
 Maoz, D., Barth, A. J., Sternberg, A., Filippenko, A. V., Ho, L. C., Macchetto, F. D., Rix, H.-W., & Schneider, D. P. 1996, *AJ*, 111, 2248
 Marconi, A., Moorwood, A. F. M., Origlia, L., & Oliva, E. 1994, *Messenger*, 78, 20
 Mathis, J. S., Rimpl, W., & Nordsieck, K. H. 1977, *ApJ*, 217, 425
 Matt, G., et al. 1996, *MNRAS*, 281, L69
 ———. 1999, *A&A*, 341, L39
 Mauder, W., Weigelt, G., Appenzeller, I., & Wagner, S. J. 1994, *A&A*, 285, 44
 McLeod, K. K., & Rieke, G. H. 1995a, *ApJ*, 441, 96
 ———. 1995b, *ApJ*, 454, L77
 McLure, R. J., Dunlop, J. S., & Kukula, M. J. 2000, *MNRAS*, 318, 693
 McLure, R. J., Kukula, M. J., Dunlop, J. S., Baum, S. A., O'Dea, C. P., & Hughes, D. H. 1999, *MNRAS*, 308, 377
 Miller, J. S., & Goodrich, R. W. 1990, *ApJ*, 355, 456
 Miller, J. S., Goodrich, R. W., & Mathews, W. G. 1991, *ApJ*, 378, 47
 Nakamoto, T., & Nakagawa, Y. 1994, *ApJ*, 421, 640
 Neff, S. G., Fanelli, M. N., Roberts, L. J., O'Connell, R. W., Bohlin, R., Roberts, M. S., Smith, A. M., & Stecher, T. P. 1994, *ApJ*, 430, 545
 Norman, C., & Scoville, N. 1988, *ApJ*, 332, 124
 Norman, C. A., & Ikeuchi, S. 1989, *ApJ*, 345, 372
 Ohsuga, K., & Umemura, M. 1999, *ApJ*, 521, L13 (Paper I)
 Ohsuga, K., Umemura, M., Fukue, J., Mineshige, S. 1999, *PASJ*, 51, 345
 Ohta, K., Yamada, T., Nakanishi, K., Kohno, K., Akiyama, M., & Kawabe, R. 1996, *Nature*, 382, 426
 Oliva, E., Marconi, A., & Moorwood, A. F. M. 1999, *A&A*, 342, 87
 Oliva, E., Origlia, L., Kotilainen, J. K., & Moorwood, A. F. M. 1995, *A&A*, 301, 55
 Omont, A., Petitjean, P., Guilloteau, S., McMahon, R. G., Solomon, P. M., & Pecontal, E. 1996, *Nature*, 382, 428
 Pier, E. A., & Krolik, J. H. 1992a, *ApJ*, 399, L23
 ———. 1992b, *ApJ*, 401, 99
 ———. 1993, *ApJ*, 418, 673
 Pérez-Olea, D. E., & Colina, L. 1996, *ApJ*, 468, 191
 Risaliti, G., Maiolino, R., & Salvati, M. 1999, *ApJ*, 522, 157
 Rix, H.-W., Rieke, G., Rieke, M., & Carleton, N. P. 1990, *ApJ*, 363, 480
 Roche, P. F., Aitken, D. K., Smith, C. H., & Ward, M. J. 1991, *MNRAS*, 248, 606
 Rodríguez-Espinoza, J. M., Rudy, R. J., & Jones, B. 1987, *ApJ*, 312, 555
 Rudy, R. J., Cohen, R. D., & Ake, T. B. 1988, *ApJ*, 332, 172
 Schiano, A. V. R. 1985, *ApJ*, 299, 24
 Schinnerer, E., Eckart, A., & Tacconi, L. J. 1998, *ApJ*, 500, 147
 Scoville, N. Z., Sanders, D. B., Sargent, A. I., Soifer, B. T., Scott, S. L., & Lo, K. Y. 1986, *ApJ*, 311, L47
 Scoville, N. Z., Sargent, A. I., Sanders, D. B., & Soifer, B. T. 1991, *ApJ*, 366, L5
 Shapiro, P. R., & Field, G. B. 1976, *ApJ*, 205, 762
 Sherman, R. D. 1979, *ApJ*, 232, 1

- Soifer, B. T., Sanders, D. B., Neugebauer, G., Danielson, G. E., Lonsdale, C. J., Madore, B. F., & Persson, S. E. 1986, *ApJ*, 303, L41
- Storchi-Bergmann, T., Mulchaey, J. S., & Wilson, A. S. 1992, *ApJ*, 395, L73
- Storchi-Bergmann, T., Raimann, D., Bica, E. L. D., & Fraquelli, H. A. 2000, *ApJ*, 544, 747
- Storchi-Bergmann, T., Rodriguez-Ardila, A., Schmitt, H. R., Wilson, A. S., & Baldwin, J. A. 1996, *ApJ*, 472, 83
- Storchi-Bergmann, T., Schmitt, H. R., & Fernandes, R. C. 1999, in *IAU Symp. 194, Activity in Galaxies and Related Phenomena*, ed. Y. Terzian, D. Weedman, & E. Khachikian (San Francisco : ASP), 295
- Storchi-Bergmann, T., Wilson, A. S., & Baldwin, J. A. 1996, *ApJ*, 460, 252
- Theis, Ch., Burkert, A., & Hensler, G. 1992, *A&A*, 265, 465
- Tomisaka, K., & Ikeuchi, S. 1986, *PASJ*, 38, 697
- . 1988, *ApJ*, 330, 695
- Umemura, M., Fukue, J., & Mineshige, S. 1997, *ApJ*, 479, L97
- . 1998, *MNRAS*, 299, 1123
- Veilleux, S., Cecil, G., Bland-Hawthorn, J., Tully, R. B., Filippenko, A. V., & Sargent, W. L. W. 1994, *ApJ*, 433, 48
- Wilson, A. S., Helfer, T. T., Haniff, C. A., & Ward, M. J. 1991, *ApJ*, 381, 79
- Wilson, A. S., Ward, M. J., & Haniff, C. A. 1988, *ApJ*, 334, 121